View metadata, citation and similar papers at core.ac.uk

brought to you by CORE

provided by Elsevier - Publisher Connector

Developmental Biology 329 (2009) 364–373

Contents lists available at ScienceDirect

Developmental Biology

journal homepage: www.elsevier.com/developmentalbiology

Genomes & Developmental Control

Similar regulatory logic in *Ciona intestinalis* for two Wnt pathway modulators, ROR and SFRP-1/5

Hélène Auger [a], Clément Lamy [b,1], Maximilian Haeussler [a], Pierre Khoueiry [b], Patrick Lemaire [b], Jean-Stéphane Joly [a,*]

[a] INRA «Morphogenèse du système nerveux des chordés» group, DEPSN, UPR2197, Institut Fessard, CNRS, 1 Avenue de la Terrasse, 91198 GIF SUR YVETTE, France
[b] IBDML, UMR6216, CNRS/Université de la Méditerranée, Parc Scientifique de Luminy, Case 907,13288 Marseille cedex9, France

ARTICLE INFO

Article history:
Received for publication 15 September 2008
Revised 22 January 2009
Accepted 3 February 2009
Available online 25 February 2009

Keywords:
Tunicate
Wnt pathway
Cis-regulation
FoxA target
Anterior ectoderm

ABSTRACT

Anteroposterior patterning of the ectoderm in the invertebrate chordate *Ciona intestinalis* first relies on key zygotic activators, such as *FoxA*, and later on the coordinated responses to inducing signals from the underlying mesendoderm. Here, we focus on a mechanism of coordination of these responses by looking at the cis-regulatory logics of *Ci-Rora* and *Ci-Rorb*, which are coding for putative non-canonical transmembrane Wnt receptors, and are present in tandem along the *C. intestinalis* chromosome 08q.

We showed that during cleavage stages, both *Ci-Rora* and *Ci-Rorb* genes are initially expressed in all blastomeres of the anterior ectoderm (a-line), as *sFRP1/5* (Lamy, C., Rothbächer, U., Caillol, D., Lemaire, P., 2006. Ci-FoxA-a is the earliest zygotic determinant of the ascidian anterior ectoderm and directly activates Ci-sFRP1/5. Development 133, 2835–2844.). We then carried out a functional analysis of *cis*-regulatory regions and showed that both genes have elements enriched in *Ci-FoxA-a* binding sites. We dissected one of these early enhancers, and showed that it is directly activated by *Ci-FoxA-a*, as one *sFRP1/5 cis*-regulatory element. We also showed that although FoxA binding sites are abundant in genomes, dense clusters of these sites are found upstream from very few genes, and have a high predictive value of a-line expression. These data indicate an important role for *FoxA* in anterior specification, via the transcriptional regulation of target genes belonging to various signalling pathways.

© 2009 Elsevier Inc. All rights reserved.

Introduction

The WNT pathway has often been separated into a “canonical” branch (beta-catenin dependent, exhaustively analyzed) and several “non-canonical” branches (beta-catenin independent, analysed more recently). Both types of pathways are essential for the regulation of numerous developmental processes and are deregulated in many human diseases (Polakis, 1997, 2007; Reya and Clevers, 2005).

In the canonical pathway, WNT signalling molecules bind to their receptor complex Lrp5/6-Frizzled receptors on the plasma membrane (Liu et al., 2005). In the “non-canonical” WNT pathway, WNT additionally binds to other receptor complexes on the membrane: RYK-Derailed, FRL-Crypto or ROR (Mikels and Nusse, 2006b). In addition, WNT molecules can also be sequestered in the extracellular space by antagonists which either bind to the signals directly (sFRPs) or block the membrane receptors (e.g. Dickkopf).

Two Ror (tyrosine-kinase orphan receptor) genes called *Ror1* and *Ror2* are found in vertebrates. They encode transmembrane receptors that bind WNT molecules and were initially thought to contribute exclusively to the non-canonical pathway (Matsuda et al., 2001; Hikasa et al., 2002; Oishi et al., 2003; Mikels and Nusse, 2006a,b; Yoda et al., 2003). These receptors are also negatively acting in the canonical pathway by providing an alternative to the Frizzled-Lrp5/6 receptor complex. ROR2 has also been shown to bind Wnt1 and Wnt3 in osteoblastic cell lines (Billiard et al., 2005); it enhances WNT-signals and interacts with Frizzled2 in lung carcinoma cell lines (Li et al., 2008). Moreover, a homolog for ROR in *C. elegans*, CAM-1, is known to inhibit the canonical WNT pathway (Green et al., 2007).

In this study, we addressed the regulation of *Ror* gene expressions in a very simple model, yet phylogenetically close to vertebrates, the ascidian *Ciona intestinalis* (Dehal et al., 2002; Blair and Hedges, 2005; Delsuc et al., 2006). Despite their small genome, *Ciona* tailbud embryos and tadpole larvae show a common body plan with vertebrate embryos: a dorsal neural tube, central notochord flanked by muscles (Satoh and Jeffery, 1995). At post-larval stages, ascidian larvae undergo an extensive metamorphosis and adults have a completely different body plan from vertebrates (Lemaire et al., 2008). *C. intestinalis* has a compact genome of only 160 Mb that contains most vertebrate transcription factor families (Imai et al., 2004). The genomic alignment

* Corresponding author.
E-mail addresses: lemaire@ibdml.univ-mrs.fr (P. Lemaire), joly@inaf.cnrs-gif.fr (J.-S. Joly).
[1] Current address: Laboratory of Molecular Developmental Biology, Department of Biophysics, Kyoto University, Kitashirakawa-Oiwake, Sakyo-ku, 606-8502 Kyoto, Japan.

0012-1606/$ – see front matter © 2009 Elsevier Inc. All rights reserved.
doi:10.1016/j.ydbio.2009.02.018

to another ascidian sequenced species, *Ciona savignyi* (Vinson et al., 2005) can be used to reduce the search space for cis-regulatory regions to the conserved regions of the genome. The functions of these latter can then be rapidly tested by electroporation (Corbo et al., 1997).

Another striking feature of ascidian embryos is their cellular simplicity and invariant cell lineages. This allows tracking the lineages up to tailbud stages. Since the work of Rose (1939) it is known that anterior and posterior ectodermal lineages of the ascidian embryo are restricted from the 8-cell stage. Recent studies found a molecular mechanism for this restriction (Okado and Takahashi, 1990; Hudson and Lemaire, 2001; Lamy et al., 2006; Imai et al., 2006) leading to the identification of *Ci-FoxA-a* as a key determinant of anterior ectodermal fate. A single direct target of *Ci-FoxA-a* in the ectoderm has been so far identified, *Ci-sFRP1/5*. However, loss of function by morpholino injection of the *Ci-sFRP1/5* gene, coding for a secreted modulator of Wnt signalling pathway has no phenotype, suggesting the presence of additional direct targets (Lamy et al., 2006).

Because of the prevalent role of canonical Wnt pathway inhibition in the acquisition of anterior ectodermal fates in vertebrates (Kiecker and Niehrs, 2001), we searched for alternative Wnt inhibitors expressed in the anterior ectodermal lineages. We examined in particular the expression patterns of the two tandemly repeated *Ror* genes, whose expressions are activated co-ordinately in the anterior ectodermal lineage. We present the dissection of the regulatory loci of the *Ror* genes. We show that conserved non-coding elements contain over-represented and functional FoxA binding sites, like *Ci-sFRP1/5*, another member of the canonical pathway. We then performed an *in silico* genome wide search for other *FoxA* targets and found them to be preferentially present in the vicinity of genes expressed in the a-lineage.

Materials and methods

Animals and embryo manipulation

C. intestinalis adults were collected at the Station Zoologique de Roscoff (Brittany, France). Embryos were obtained by *in vitro* cross-fertilization in artificial seawater as described before (Hudson and Lemaire, 2001). Single cell zygotes were dechorionated according to Mita-Miyazawa et al. (1985). For in situ hybridization, bacterial clones were picked from the *C. intestinalis* gene collection release 1 (Satou et al., 2002). Digoxigenin-labelled antisense or sense RNA probes were synthesized from the following cDNAs: *Ci-Rora* (ci0100130024) and *Ci-Rorb* (ci0100130025), and purified (Nucleospin mRNAII purification, Macherey-Nagel). Probes were hybridized to embryos using an In situ Pro automat (Intavis), as described in Deyts et al. (2005). They were treated with proteinase K (2 μg/mL, 30 min at 37 °C). Hybridized embryos and vibratome sections were observed under an SV11 Zeiss dissecting microscope or a Leica DRM microscope. Images were recorded with a Nikon DXM 1200 digital camera.

Electroporations and X-Gal stainings were performed as previously described (Corbo et al., 1997; Bertrand et al., 2003). Living embryos, juveniles and neural complexes dissected were observed under a Zeiss Axioplan 2 imaging. *Ci-FoxA-a* over-expression by electroporation was performed as described in Lamy et al. (2006).

Sequence comparison and analysis

C. intestinalis and *C. savignyi* genomic sequences were obtained from the JGI (Dehal et al., 2002) and from the Broad Institute (http://www.broad.mit.edu/annotation/ciona/), respectively, and handled with the Vector NTI Suite (Informax). The VISTA algorithm (Frazer et al., 2004) was used for sequence alignment and comparison with the following parameters: 100 bp windows, 70% identity threshold. Conserved Non-coding Sequence (CNS) boundaries were refined by local alignment.

For the phylogenetic analysis, multiple protein sequences were aligned using ClustalX, with manual optimization (Thompson et al., 1997) using MUST software (Philippe, 1993). Regions of ambiguous homology were removed. We then calculated the maximum likelihood (ML) trees using PHYML (Guindon and Gascuel, 2003). The robustness of the ML trees was estimated by 100 bootstrap replications.

Molecular cloning and dissection of Ci-Ror-a and Ci-Ror-b genomic fragments

Ci-Rora and *Ci-Rorb* cis-regulatory fragments were amplified by PCR from *C. intestinalis* sperm genomic DNA using Accuprime HiFi Taq Polymerase (Invitrogen) and inserted in p1.72BSSPE/ISceI/RfA-Venus, p1.72BSSPE/ISceI/RfA:H2B:EGFP or p1.72BSSPE/RfA:NLS-lacZ Gateway destination vectors. These vectors are derived from a set of vectors for ascidian transgenesis (Roure et al., 2007) by addition of I-Sce1 sites to make them compatible with the meganuclease mediated transgenesis in fish (Thermes et al., 2002) thus allowing inter-species analyses. A precise map of these vectors is available on the AMAGEN web site (http://amagen.inaf.cnrs-gif.fr/fr/vecteurs). To test enhancer activities, genomic sequences were amplified by PCR, Gateway cloned into pDONR-221-P3-P4 vector and the resulting entry clones recombined into pSP72BSSPE-R3-ccdB/cmR-R5::B1-NLSlacZ-B2. The destination vectors were electroporated as described (Bertrand et al., 2003, $n>100$ and at least 2 independent experiments for each condition). Specific sequences of the primers used to clone the different genomic fragments are listed in Supplemental Fig. 1.

In silico analysis of FoxA binding sites

The *Ci-Rora* and *Ci-Rorb* regulatory regions were analysed by phylogenetic footprinting using Vista (http://genome.lbl.gov/vista/) (Frazer et al., 2004). (http://www.generegulation.com/pub/databases.html) (Matys et al., 2003).

Putative Fox binding sites were first searched using UCSC genome browser. A plot of non-exonic matches for TGTTT to the VISTA-plot is added to illustrate this search in Fig. 1. We searched the sequence of 50 kb shown in Fig. 1 of *C. intestinalis* for matches with the consensus TGTTT.

For whole-genome analyses, we downloaded the assembly version 2 for *C. intestinalis* from the UCSC genome browser website and Version 2 of *C. savignyi* from Ensembl and ran tandem repeat masker on the latter genome. All pairwise alignments between all scaffolds of the two species were calculated with BLASTZ, followed by the chaining-netting process as explained in Saitou and Nei (1987). We have documented the procedure in detail at http://genomewiki.cse.ucsc.edu/index.php?title=Whole_genome_alignment_howto&oldid=4704. We then annotated the genome with the positions of JGI1 gene models using BLAT and removed all conserved regions that overlapped exons with the UCSC table browser. This led to an alignment which covers 26 MBbp out of the 141 MBbp of the total genome of *C. intestinalis*. Every locus in *C. intestinalis* is aligned to a single locus in *C. savignyi* when the repeated regions are removed. Alignments were then processed with a script (maf2words) which converts every conserved block into a consensus sequence and keeps only pentamers and their associated positions.

A second script (motifEvaluator) searches all conserved consensi for all possible pentamers which match 3 times within a window of 250 bp. The positions of all word-matches are annotated with both flanking genes which results in a list of genes flanking the matches for every motif.

Results and discussion

Ror genes, protein structures and phylogenetical relationships

We used the JGI2 and the KyotoGrail genome browsers to define the genomic structure of the two Ror genes. *Ci-Rora* and *Ci-Rorb* are

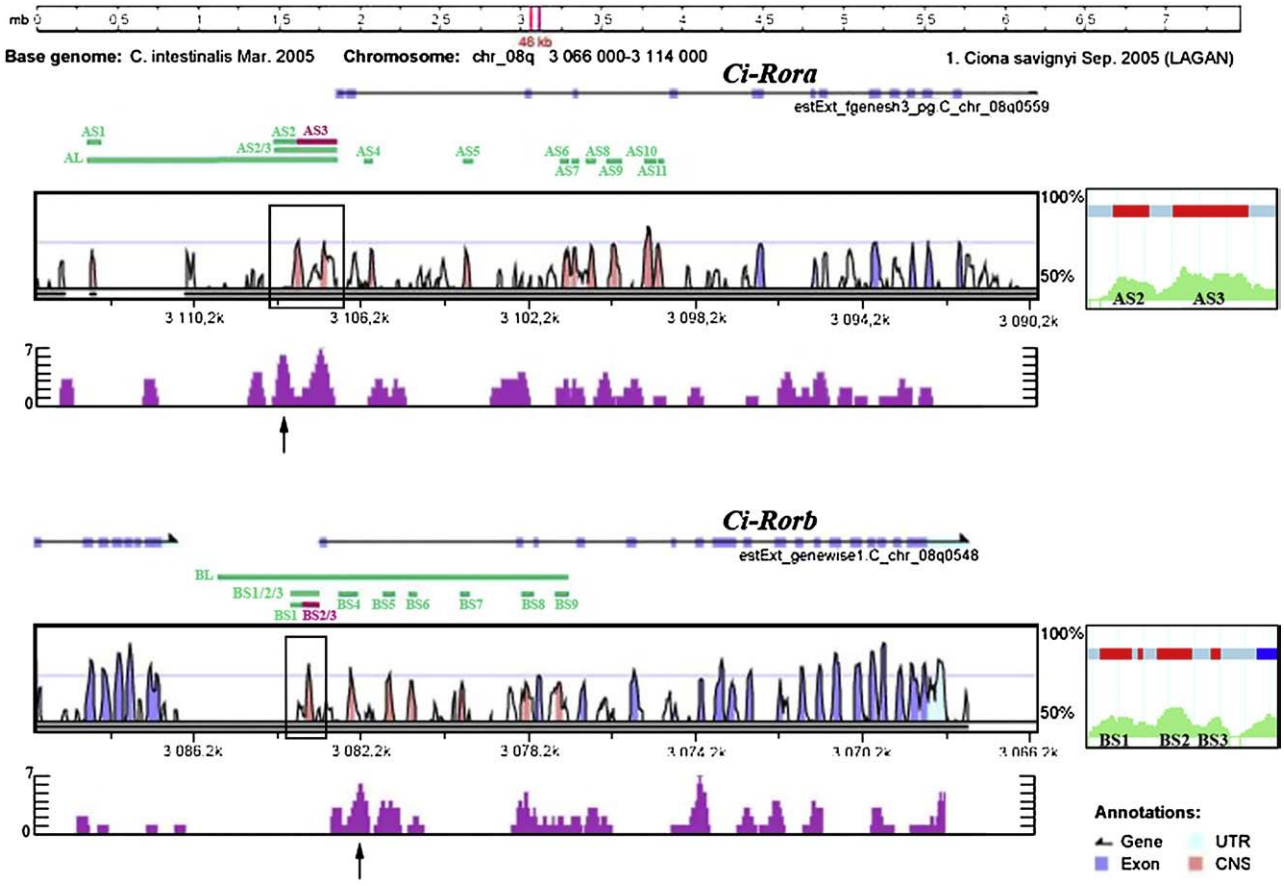

Fig. 1. Locus of *Ci-Rora* and *Ci-Rorb*, tandem genes in direct sense, in the *Ciona intestinalis* genome. VISTA plot (percent identity with *Cs-Ror* genes) and schemes showing the position of the different constructs tested in vivo for *Ci-Rora* (AL, AS1, AS2, AS3 and AS2/3) and *Ci-Rorb* (BL, BS1, BS2/3, BS1/2/3 and BS4). A plot of non-exonic matches for TGTTT in a 250 bp window in *Ciona intestinalis* non-coding regions has been added to the VISTA-plot (in pink). The 2 black arrows show the *Rora* AS2 enhancer containing 5 FoxA sites and the *Rorb* BS4 enhancer containing 6 FoxA sites. The two panels on the right show a detailed view of the conservation (in green) of the AS2/AS3 and BS1/BS2/BS3 fragments (boxes in the alignment).

localised in tandem in direct direction (Fig. 1). They are each composed of 19 exons distributed on 20 kb for *Ci-Rora* and 14 kb for *Ci-Rorb*. They encode transmembrane receptor tyrosine kinase-like orphan receptors containing an Ig-like (IGc2), a kringle and a Frizzled-like domains. The latter constitutes the extracellular ligand-binding region of *frizzled* receptors, known to bind WNT family members.

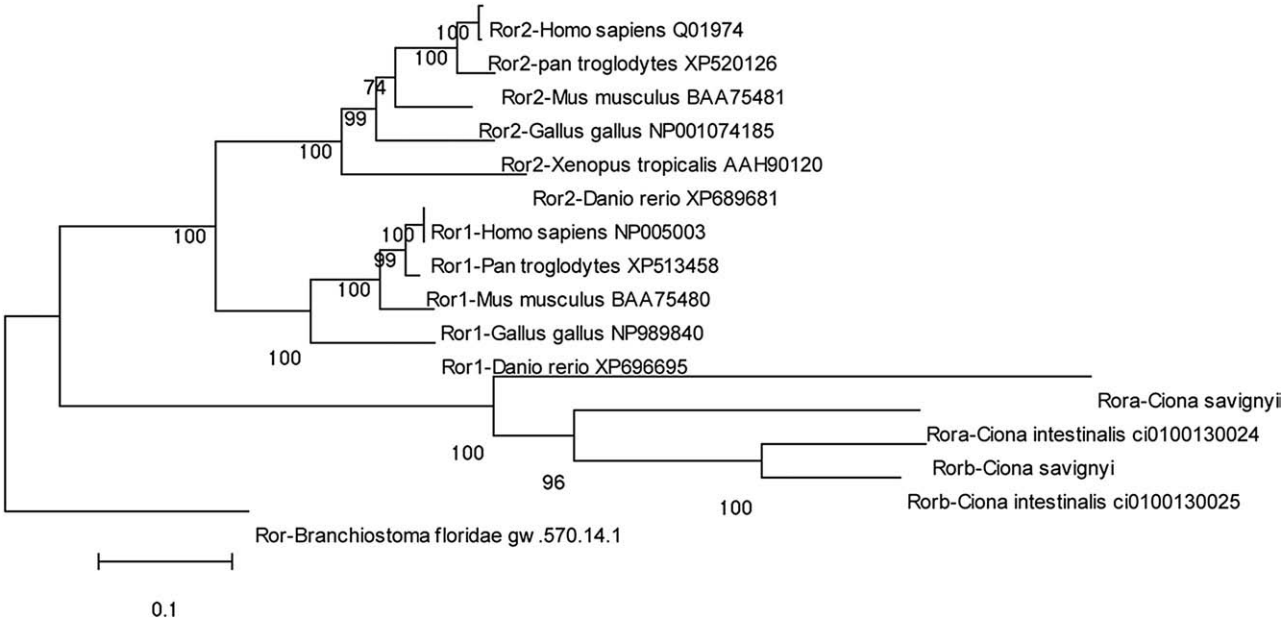

Fig. 2. Phylogeny of the Ror proteins reconstructed by the neighbor-joining method. The main observation is that the two *Ciona Ror* genes are phylogenetically closely related and do not fall within any specific vertebrate clade. So *Rora* and *Rorb* genes are not orthologous to *Ror1* and *Ror2* genes in vertebrates. Species are indicated after gene names.

To infer the evolutionary relationships between invertebrate chordate and vertebrate ROR proteins, we compared the shared molecular features of the vertebrate ROR proteins and other deuterostomian genomes, including tunicates or cephalochordates. Fig. 2 depicts the genealogy of the Ror genes, reconstructed by the neighbour-joining method applied to the proteins sequences (Guindon and Gascuel, 2003).

The neighbour-joining tree divides the genealogy into three major clades. One clade comprises the vertebrate proteins. Another one comprises the *Ciona* ROR proteins, whereas the deduced amphioxus proteins root the trees. The two *Ciona* ROR proteins are phylogenetically closely related. Moreover, the proteins from the *Ciona* genomes do not fall within any specific vertebrate clade. Because they form a tandem duplicate, we propose that *Ror* genes experienced a duplication in the lineage leading to extant ascidians. So *Rora* and *Rorb* genes are not orthologous to *Ror1* and *Ror2* genes in vertebrates. These two later vertebrate genes probably arose in the course of whole genome duplication events in the vertebrate lineage (Jaillon et al., 2004).

Ci-Rora and Ci-Rorb are two anterior markers

To compare *Ci-Rora* and *Ci-Rorb* expression patterns with those of the main actors of the Wnt canonical pathways, we first studied expression patterns by whole-mount *in situ* hybridisations (WMISH) in a more detailed way than in Bertrand et al. 2003, where one *Ror* gene was reported to be expressed in the anterior neural plate (Fig. 3).

Onset of *Ci-Rora* expression was observed at the 32-cell stage in the a6.5 to a6.8 blastomeres. This expression intensified and persisted in all anterior animal blastomeres until the 110-cell stage. During gastrulation, expression of *Ci-Rora* became progressively restricted to the a-line blastomeres of the neural plate, derived from the a7.9, a7.10 and a7.13 blastomeres (Nishida and Satoh, 1985). By the neural plate stage (Hotta et al., 2007; Christiaen et al., 2007), *Ci-Rora* remained only expressed in the 4 anterior-most rows of cells of the neural plate (row III to VI). During neurulation, the neural plate elongates along the AP axis, as a result of oriented cell divisions (Nishida and Satoh, 1985; Passamaneck et al., 2007). During this developmental period, a second wave of extinction of *Ci-Rora* expression in the neural a-line

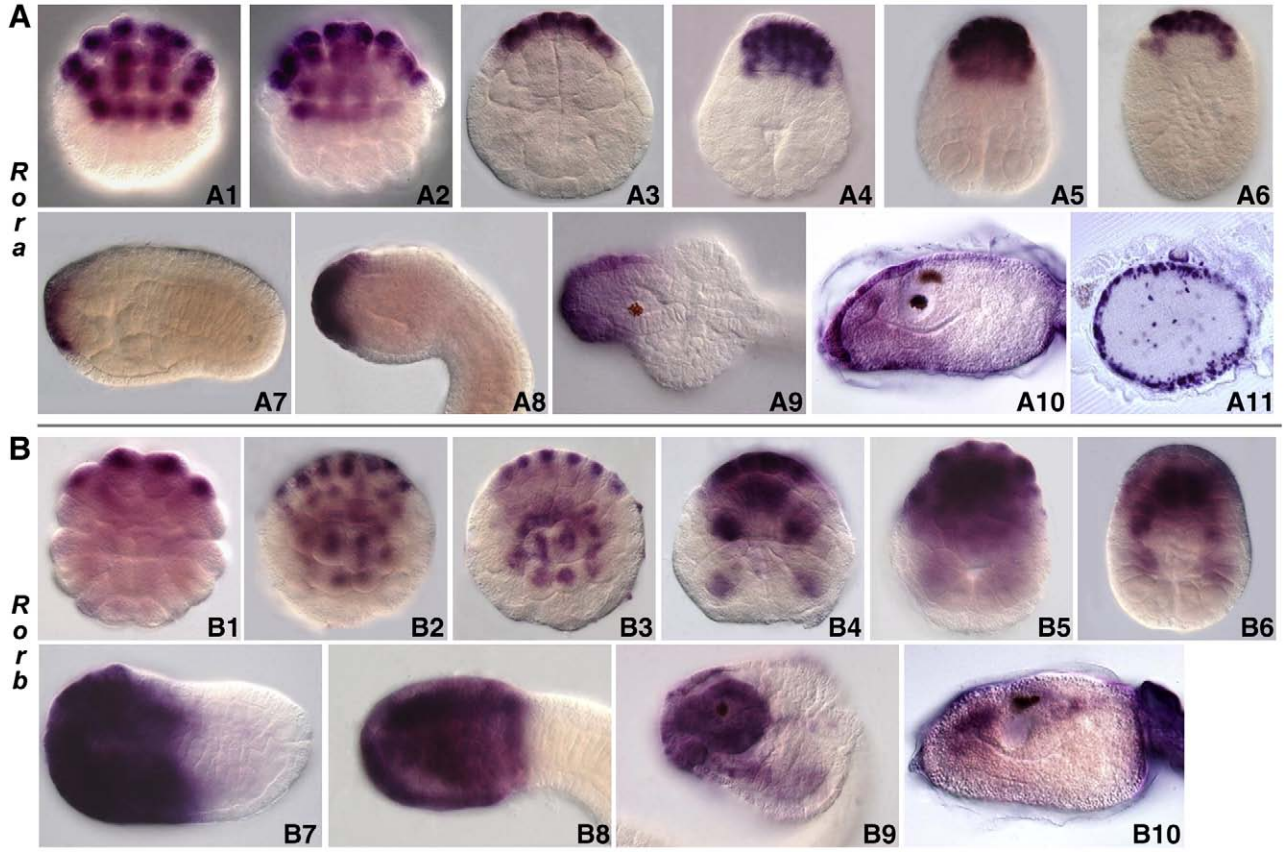

Fig. 3. Temporal and spatial expression pattern of *Ci-Rora* (A) and *Ci-Rorb* (B), as revealed by WMISH. (A1–A2) Segmentation stages in animal view. *Rora* is expressed in the a-line blastomeres at the 64-cell stage (A1) and 110-cell stage (A2). (A3–A5) From the gastrula stage to the mid neurula stage, *Rora* expression is restricted to the neural a-line blastomeres. (A3) gastrula stage in animal view, (A4) 40-cells neural plate stage in animal view, (A5) neurula stage in animal view (A6) At the late neurula stage in animal view, we observed that *Rora* expression is then restricted to the anterior epidermal a-line blastomeres. *Rora* goes on being expressed in the rostral neural tissues and in the head epidermis from tail-bud to larval stages (A7–A10) onwards. (A7) In early- or mid-tailbud embryos, the most anterior part of the head epidermis and a row of cells called the stomodeal placode are stained. (A8–9) In late-tailbud stages, the stomodaeum forms and still expresses *Rora*. Also, the anterior part of the sensory vesicle, the ascidian forebrain, is stained. Expression in the anterior epidermis is restricted at this stage to the presumptive domain of the palps. It is likely that this expression is found in derivatives of the formerly more dorsal epidermal cells at early-tailbud. (A10) At the larval stage, we have observed an expression reminiscent of the one found in tailbud embryos one: *Rora* in the palps, in the anterior epidermis (dorsal and ventral) and in the anterior sensory vesicle (dorsal stomodaeum). (A11) Later in the adult, on vibratome sections of the neural complex, *Rora* is clearly expressed in the cortex of the ganglion (where many cell-bodies are gathered) and in the ciliated duct that connect the neural gland to the dorsal tubercle. All along the development, *Rorb* is expressed in the a-line blastomeres that will give rise to the anterior nervous system and anterior epidermis. (B1) 64-cell stage in animal view, (B2) 110-cell stage in animal view, (B3) 110-cell stage in vegetal view, (B4) gastrula stage in animal view, (B5) 40-cells neural plate stage in animal view, (B6) neurula stage in animal view, (B7) early-tailbud stage in lateral view, (B8) mid-tailbud stage in lateral view, (B9) late-tailbud stage in dorsal view, (B10) larval stage in lateral view. At the late tail-bud stage (B9), the distribution of *Ci-Rorb* transcripts showed a rostral restriction within the anterior epidermis and nervous system, as well as in the anterior endoderm. However, its expression is less dynamic that the *Ci-Rora* one. At larval stage (B10), the expression of *Ci-Rorb* is then restricted to the rostral part of the sensory vesicle, the deep domain of the stomodaeum and a week expression is seen in the most anterior area of the head endoderm. Contrasting with *Ci-Rora*, *Ci-Rorb* is not found expressed in the adult neural complex on vibratome sections.

progenitors starts from the posterior region. In contrast, anteriorly to the plate, epidermal a-line progenitors begin expressing *Ci-Rora*. Expression is thus very dynamic at that stage.

We next studied the expression of *Ci-Rorb* and compared it to the highly dynamic *Ci-Rora* expression. *Ci-Rorb* is first expressed in all a-line blastomeres at the 64-cell stage. Then, at the 110-cell stage, in addition to all a-line blastomeres, *Ci-Rorb* is expressed in all endodermal progenitors, like *Ci-FoxA-a* (Corbo et al., 1997). At all the gastrula stages, *Ci-Rorb* is expressed in the neural and epidermal a-line. We also observed at these stages two bilaterally symmetrical spots of *Ci-Rorb* expression corresponding to the endodermal progenitors. During neurulation, *Ci-Rorb* is expressed in the precursors of the anterior epidermis, in the most rostral rows of the neural plate, and in the invaginated precursors of the anterior endoderm. Its ectodermal expression is quite similar to the *Ci-Rora* one at this stage. This is in contrast with the situation observed soon after. Indeed, in late neurula early-/mid-tailbud stage, we observed that *Ci-Rorb* remains strongly expressed throughout the head epidermis as well as in the developing nervous system (whole sensory vesicle and stomodaeum). Again, *Ci-Rorb* is expressed in anterior endodermal tissues that have reached the anterior region of the head.

Our expression pattern study thus unravelled co-expression of the two *Ci-Ror* genes and *Ci-sFRP1/5* during cleavage stages. During the gastrula and neurula stages, while *sFRP1/5* and *Rorb* retain expression throughout the a-line, *Rora* shows a more dynamic expression pattern in the ectoderm.

Like many tandem duplicated genes the two *Ci-Ror* genes thus show many common domains of expression and some differences mainly at late stages. Although we cannot exclude that these differences rely on post-transcriptional mechanisms, we chose in this paper to explore the transcriptional regulation of the two genes to explain the similarities as well as the differences they display.

Exploring the non-coding regions flanking Ci-Ror genes

To identify the *cis*-regulatory regions driving *Ci-Ror* genes expression, the spatiotemporal transcriptional activity of two genomic fragments located in the 5′ flanking regions of each gene was assessed by electroporation (Fig. 4). One of these long fragments (AL; 4 kb) maps upstream of the *Ci-Rora* gene. The other (BL; 7.9 kb) includes the intergenic sequence between *Ci-Rora* and *Ci-Rorb* and the three first introns of *Ci-Rorb*. AL and BL do not overlap (Fig. 1).

The AL fragment recapitulates most of the endogenous expression pattern of *Ci-Rora* during segmentation, gastrulation and neurulation. EGFP fluorescence is first detected in all a-line blastomeres at the 110-cell stage, two cleavages after the onset of expression of the endogenous gene (Fig. 4, A1). This delay may reflect the time necessary for the EGFP protein to mature, as we revealed performing an in situ hybridization against EGFP whose expression mimicked the endogenous transcript patterns (data not shown). During gastrula stages, as described above for the endogenous expression pattern, EGFP expression is restricted to the neural a-line blastomeres (Fig. 4, A2). At the neural plate stage, EGFP expression is still observed in the progenies of the expressing blastomeres at the early gastrula stages (Fig. 4, A3). At the early-tailbud stage (Fig. 4, A4) AL-driven activity becomes more widespread than the endogenous expression in the head epidermis and in the anterior nervous system (sensory vesicle). At late-tailbud (Fig. 4, A5) and larval stages (Fig. 4, A6), AL activity is detected in the most rostral part of the head epidermis, in the anterior part of the nervous system (sensory vesicle, stomodaeum) and in the palps. As reported above, expression of *Ci-Rora* undergoes several waves of restriction at these stages, and in contrast, the more stable EGFP protein remains in the derivatives of the early expression domains. No expression was detected after metamorphosis in the adult, in contrast with the endogenous *Rora* expression pattern detected in the ganglion and in the ciliated funnel (Fig. 3, A11).

Many non-coding conserved sequences are found in the BL fragment. However, in BL electroporated embryos, we could only detect Venus expression after metamorphosis of the transgenic larvae. The transient expression was in the primordium of the dorsal tubercule and in the tip of the endostyle. In the adult, the signal was found in the ciliated funnel and at the tip of the endostyle (Fig. 4C).

We conclude that long flanking regions of the *Ci-Rora* and *Ci-Rorb* genes contain most of the critical elements to drive early and late expressions of the genes. While early elements are found in the upstream regions from the tandem genes, late elements seem to be found in the intergenic region, downstream of *Rora*, which is expressed in the ganglion and the ciliated funnel.

Characterisation of the activity of short proximal conserved elements

Next, we sought to identify shorter regulatory elements regulating *Ci-Ror* genes with a special emphasis on early expression from blastula to early-tailbud stage. Conserved non-coding sequences between the genomes of *C. intestinalis* and *C. savignyi* can help predict functional elements (e.g., Frazer et al., 2004). To identify short regulatory elements within the AL and BL fragments, we used the VISTA algorithm to perform inter-specific sequence comparisons within 50 kb of the *Ci-Ror* loci (Fig. 1). The *Ci-Rora* upstream region contains three short (S) highly conserved regions: a distally located one (called AS1, 4 kb upstream from the putative transcription start site, 95 bp) and two proximal ones (AS2 and AS3, 120 bp and 130 bp respectively) located just in front of the transcription start site.

The intergenic region located between the two *Ror* genes exhibits three highly conserved fragments (BS1 to 3) placed side by side. The region overlaps the *Ci-Rorb* putative transcription start site and first exon, and extends 700 bp upstream from these. Like *Ci-Rora*, the first three *Ci-Rorb* introns are also rich in highly conserved sequence blocks (BS4 to BS9).

We first paid attention to the location of the transcription start sites. We could not identify in the EST data any splice leader tag such as the ones identified by Satou et al., 2006, indicating that no trans-splicing occurs. Thus, the transcription start sites are likely to be located just upstream of the two genes as indicated by the 'Ciona Filtered Models V2.9' from the JGI V2.0, a hypothesis strengthened by EP3 promoter predictions (http://bioinformatics.psb.ugent.be/webtools/ep3/; Abeel et al., 2008).

We first tested the proximal elements found upstream of the transcription start sites. A construct was made, in which a Histone 2B-EGFP fluorescent reporter was placed downstream of the proximal elements AS2/3. This element with two conserved blocks was found to be active in the same domains as AL (Fig. 4A), recapitulating the endogenous expression pattern of *Ci-Rora* (as checked by ISH on GFP transcripts, not shown). AS2/3-driven transient expression starts at the 110-cell stage, in the a-line blastomeres and is restricted at the gastrula and neural plate stages to the neural a blastomeres. Then it becomes expressed at the tailbud stages and at the larval stage in the most anterior part of the head epidermis and nervous system (sensory vesicle, stomodaeum and palps).

We next tested a construct corresponding to the BS1/2/3 fragment located upstream of *Rorb*. Although no expression was detected in endodermal cells, where *Ci-Rorb* is expressed, BS1/2/3 drove EGFP expression in several anterior domains of the electroporated embryo trunks. BS1/2/3 is indeed active in the a-line blastomeres from the 110-cell stage to the larval stage, with a pattern mimicking the endogenous gene (Fig. 4B). However, at early- and mid-tailbud stages (Fig. 4, B3–4), EGFP was restricted to the posterior part of the head epidermis in a consistent way with the weak epidermal expression during late neurula stages. At late-tailbud stage (Fig. 4, B4), BS1/2/3

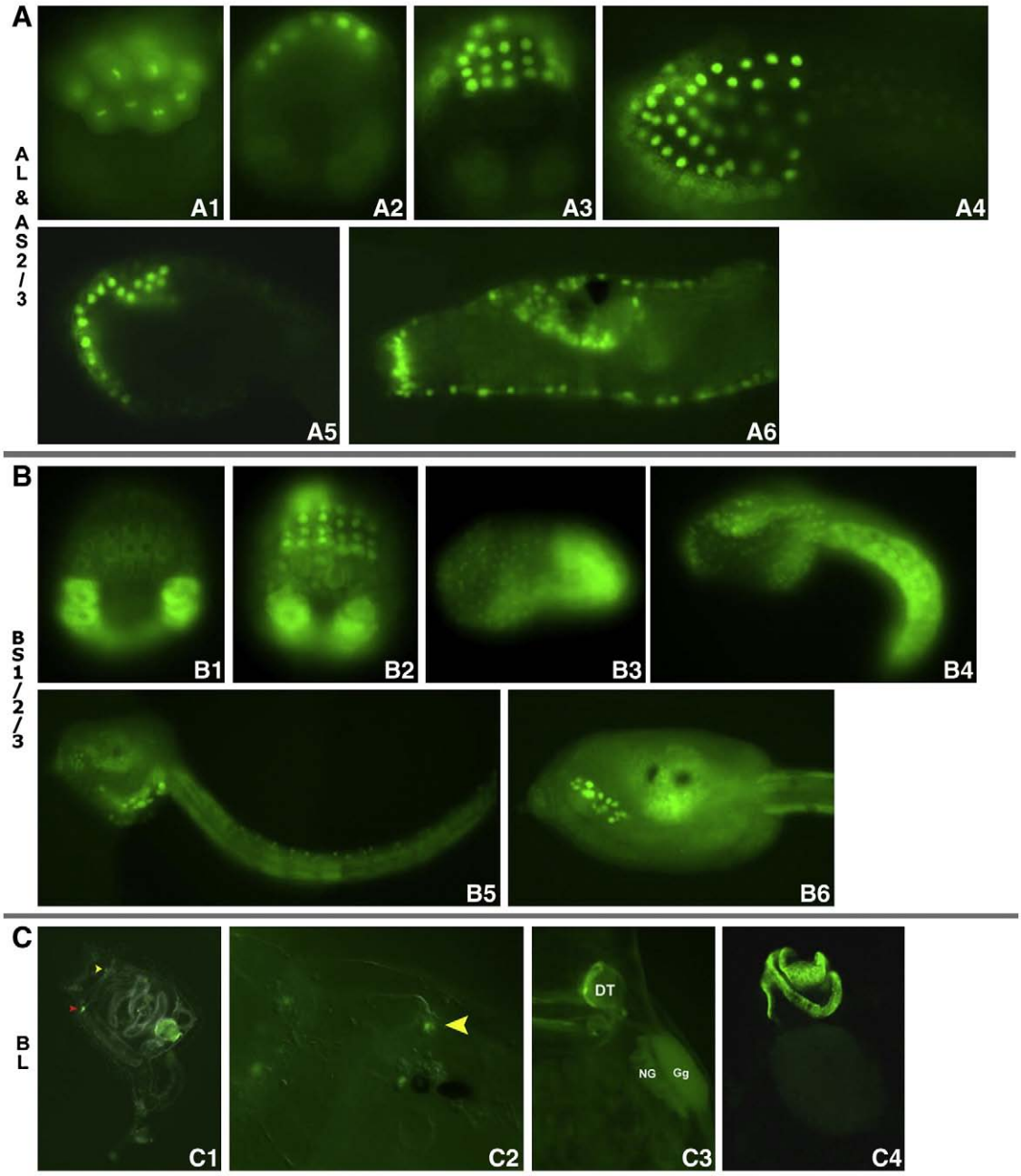

Fig. 4. (A) Nuclear and transient expression of AL::*H_2B EGFP* and AS2/3::*H_2B EGFP* constructs in electroporated *Ciona* embryos at different developmental stages. The 2 constructs recapitulate the endogenous expression pattern of *Ci-Rora* in the a-line blastomeres. (A1) 110-cells stage, (A2) gastrula stage. (A3) 40-cells neural plate stage, (A4) early-tailbud stage. At this stage, the transient expression is more widespread than the endogenous expression of *Ci-Rora*, due to the stability of the EGFP protein. (A5) mid-tailbud stage, (A6) larval stage. (B) Nuclear and transient expression of the BS1/2/3::*H_2B EGFP* construct. The BS1/2/3 construct recapitulates the endogenous expression pattern of *Ci-Rorb* in the a-line blastomeres (but not in the endodermal blastomeres), except that the transient expression starts later than the endogenous expression (40-cells neural plate stage instead of 64-cells stage). We can observe a strong autofluorescence in the tail muscles progenitors, as seen in (B1) on a negative embryo at early neural plate stage. (B2) 40-cells neural plate stage, (B3) early-tailbud stage, (B4) late-tailbud stage, (B5, B6) young larvae. (C) Cytoplasmic expression of the BL::*Venus* construct. The BL fragment drives a transient expression only after metamorphosis and in the adult. (C1) young juvenile showing a transient expression of the BL construct in the primordium of the dorsal tubercle (DT) (yellow arrowhead) and at the tip of the endostyle (red arrowhead). (C2) High magnification oh the primordium of the DT. (C3) Neural complex of a transgenic BL::*Venus* animal. The expression is seen in the ciliated funnel placed side to the DT. (NG) neural gland, (Gg) cerebral ganglion. (C4) Dissected neural complex of a transgenic BL::*Venus* animal. Strong transient expression in the ciliated funnel.

was found to be active at least in the head epidermis, in the sensory vesicle and in the presumptive domain of the palps, like the endogenous *Ci-Rorb*.

These results provided stimulating cues for the presence of both enhancers and core promoters in the proximal AS2/3 and BS1/2/3 short elements. The latter result is surprising as the BL fragment at these stages lacked activity and suggests that this later may include strong repressor elements.

Further dissections of the short proximal cis-regulatory elements

To further identify which parts of the AS2/3 and BS1/2/3 elements constitute enhancers and basal promoters, we performed two types of experiments. We first assayed distal fragments for enhancer activity by placing them in front of the basal promoter of the *FOG* gene and a nuclear beta-galactosidase reporter gene. We also examined whether proximal or distal fragments alone could drive *lacZ* expression. All

constructs were electroporated into *C. intestinalis* fertilized eggs and the reporter activity was assayed by X-Gal staining during cleavage and mid-tailbud stages.

AS2 placed upstream of the FOG basal promoter has a similar activity as AS2/3 in the anterior ectoderm (neurectoderm and epidermis) (Fig. 5A). In contrast, when placed alone in a destination vector containing no basal promoter the AS2 and AS3 elements did not drive any expression (not shown). This could indicate that the AS3 element, which contains the closest conserved sequence to the transcription start site, is a basal promoter.

We then performed similar experiments to dissect BS1/2/3. When placed in front of the *FOG* basal promoter, BS1 drove a strong

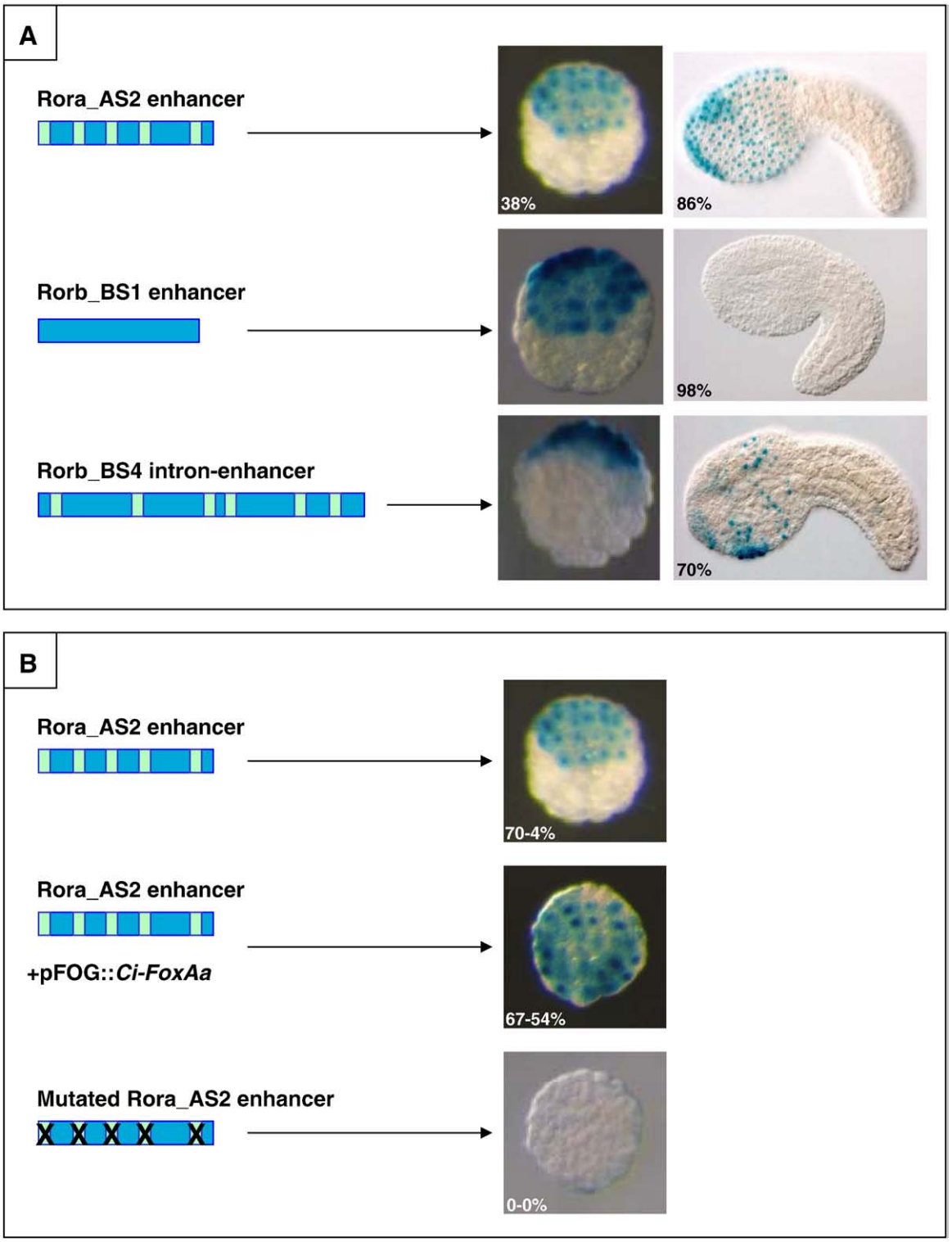

Fig. 5. Different enhancers in front of a *FOG* basal promoter were electroporated in *Ciona* eggs. (A) Representative X-gal embryos are shown at the 110-cell and tailbud stages for *Rora* AS2 enhancer, *Rorb* BS1 enhancer and *Rorb* BS4 intronic enhancer constructs. The percentage of embryos with a-line staining is indicated. (B) *Ci-Rora* is a target of *Ci-FoxA-a* via its AS2 enhancer *Ci-FoxA-a* overexpressed and Fox-mutated embryos at the 110-cell stage. Percentages indicate staining in a-line and b-line respectively. 110-cell stage embryos are in animal view, anterior to the top; tailbuds are in lateral view, anterior to the left, dorsal to the top.

expression in all a-line blastomeres (neural and epidermal) at the 110-cell stage, but surprisingly, no expression was driven at the tailbud stage (Fig. 5A). This element is thus an early enhancer active in the anterior ectoderm, but in contrast to the *Rora* AS2 enhancer previously described, it has no activity later in development. Similarly, BS2/3 in front of a *LacZ* reporter gene did not drive any expression, indicating that this element does not contain the information required to drive *Ci-Rorb* expression. Similarly to AS3, we suggest that the BS2/3 element is a basal promoter.

Characterisation of regulatory elements with dense FoxA binding site clusters

Because a perfect correlation between the presence of dense clusters of Fox-binding sites and the ability of the fragment to drive pan-a-line is found in *sFRP1/5 cis*-regulatory elements (Lamy et al., 2006), we performed manual and *in silico* searches for Fox-binding sites. It may be noted here that many other FOX proteins share similar binding affinities to DNA but because of its animal expression in the a-lineage *FoxA-a* appears as the best candidate. In Lamy et al. (2006), authors looked for TGTTT sites. The consensus of the known FoxA binding sites is indeed TG/ATTT (Overdier et al., 1994) and it has been reported that TGTTT sites are bound with higher affinity by *FoxA* during early development in *C. elegans* (Gaudet and Mango, 2002).

The VISTA software also revealed many clusters of putative Fox-binding sites in the vicinity of *Rora* coding sequence (Fig. 1). Among these, the AS2 element contains 5 TGTTT and is present in the AL fragment driving early expression. We cloned this sequence in front of the *FOG* basal promoter and a *LacZ* reporter gene. The construct was electroporated in fertilized *Ciona* embryos, and the resulting activity was visualized at the 110-cell and mid-tailbud stages by X-gal staining. A strong staining was observed in the anterior ectodermal lineage for the *Ci-Rora* AS2 enhancer at the 110-cell and tail-bud stages. This pattern is somewhat different from the endogenous *Rora* expression that becomes restricted to the a-line blastomeres at the neurula stage.

Then, we tested the role of the Fox-binding sites by point mutating (TGTTT → TGCTT in each motif) them in the AS2 element. The resulting construct showed no activity after electroporation and staining at the 110-cell stage (Fig. 5B) as well as at the tailbud stage (data not shown).

Ci-FoxA-a is known to be a global determinant of anterior ectoderm (Lamy et al., 2006). To address whether *Ci-FoxA* activates the expression of *Ci-Rora* via the AS2 element, we overexpressed *Ci-FoxA-a* in all animal blastomeres by electroporating pSP1.72-pFOG::*Ci-FoxA-a*. In the electroporated embryos, ectopic staining for anterior markers (including *Ci-Rora*) had already been observed at the neural plate stage in b-line cells (Lamy et al., 2006). When the AS2 element was co-electroporated with the *Ci-FoxA* over-expression construct, ectopic lacZ activity was observed throughout the ectoderm of manipulated embryos (control embryos 4%, $n=56$; *FoxA-a* over-expressed embryos 54%, $n=53$) (Fig. 5B). These two experiments indicate that Fox sites are necessary for AS2 early enhancer activity and that FoxA-a protein is sufficient to activate *Ci-Rora* AS2 in whole ectoderm.

A second cluster was found in a sequence of 249 bp corresponding to the *Ci-Rorb* BS4 element containing 6 putative Fox-binding sites, localized in the first intron of the *Ci-Rorb* gene and in the BL region. Because BL did not drive any early expression, we did not perform a detailed analysis of this element but just checked if this element would have an early activity in the a-line. Surprisingly the *Ci-Rorb* BS4 intronic enhancer construct (Fig. 5A) showed a restricted staining in the a-line blastomeres. Not all epidermic a-line blastomeres were stained at the 110-cell stage whereas all the neural a-line blastomeres were stained. At the tailbud stage, on the contrary of the endogenous expression pattern, not all epidermic cells of the head were stained. This result confirmed that the BL fragment may include strong repressor elements.

We conclude that, like the *Ci-sFRP1/5* enhancer, the *Ci-Rora/Rorb* enhancers are likely targets of *Ci-FoxA-a* in the anterior ectoderm.

Clusters of Fox-responsive elements are rare in Ciona genomes and putatively activate gene expression in the a-line

Because the AS2 element has 5 TGTTTs, we decided to examine if such clusters are abundant in intergenic sequences that are conserved between *C. intestinalis* and *C. savignyi*. The distribution of the lengths of conserved non-coding sequences in the genome shows a peak around 250 bp (Supplemental Fig. 2). So, we used a window size of 250 bp and searched all non-coding sequences for 5 conserved matches of TGTTT within this window. Strikingly, we could identify a very low number of 14 other conserved-non-coding regions with 5 or more TGTTT indicating that very few genes have so dense clusters of Fox-binding sites in their flanking regions.

As this binding site density is clearly too high to reveal all potential *FoxA* targets in the genome, we lowered the constraint to 3× TGTTT over 250 bp. In order to show that conserved regions containing 3× TGTTT preferentially flank a-line specific genes, it is necessary to compare two types of data: 1) genes that are expressed in the a-lineage and 2) genes that contain 3× TGTTT in their conserved non-coding regions. For 1) we downloaded a list of genes expressed in the animal region at the 64-cell and/or 110-cell stages from the ANISEED database (http://aniseed-ibdm.univ-mrs.fr). We found 234 annotated genes corresponding to our criteria. 21 of those are expressed in the a-line but not in the b-line at the 64-cell and/or 110-cell stages. We ignored expression in the A or B lineages and call these 21 genes "a-line expressed genes" (listed in Supplemental Table 1).

For data of the type 2) – genes that are located close to a TGTTT-cluster – we searched the genome for 3 or more conserved copies of TGTTT within 250 bp in regions conserved between *C. intestinalis* and *C. savignyi*. This resulted in 489 matches flanking 575 genes. The list includes homologs of known human WNT components, such as Dickkopf, WNT9, WNT6, WNT7, ROR, SFRP1 and Prickle (see Supplemental Table 2). Among the 575 flanking genes, 34 (out of 234 genes with annotated expressions in ANISEED) are expressed at the 64-cell and/or 110-cell stages and 8 of these 34 genes are specific of the a-line (Fig. 6).

To see if the number 8 is significantly different from what would be expected by chance, we used the hypergeometric distribution, inspired by Hughes et al. (2000). The probability to find 8 or more positive genes by chance when randomly drawing, without replacement, 34 from 234 genes of which 21 are positive and 213 are negative is 0.004504. We conclude that the list of genes flanked by conserved regions containing 3× GTTT is significantly enriched in regions flanking genes expressed in the a-lineage (Fig. 6).

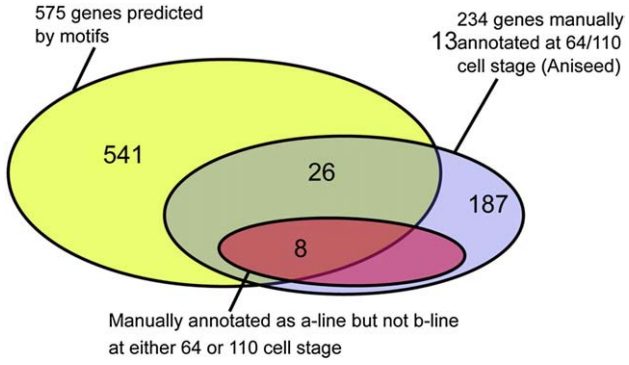

Fig. 6. Overlap between the set of genes flanked by clusters of conserved putative FoxA binding sites found in our genomic analysis and the set of a-line expressed genes as annotated in the Aniseed database.

Of the four nucleotides A/C/T/G, one can build 512 different pentamers. To show that no other motif-trimer within 250 bp predicts the a-lineage better, we have repeated the procedure applied to the TGTTT pentamer for all possible 512 pentamers, then ranked the motifs by their *p*-value. A striking result was that we could not find three copies of any pentamer that predict the a-lineage better than TGTTT.

These *in silico* studies thus suggest that clusters of FoxA binding sites are key features to regulate target genes in anterior ectoderm. We show here that key target genes belong to various signalling pathways, a result in contrast with other studies on liver cells showing that FoxA clusters probably have targets associated with cell proliferation.

We have found that there are enhancers with similar logics consisting in the presence of repeated FoxA binding sites around the duplicated *Ci-Rora/b*. However, it should also be noted that one of the active elements called BS1 does not appear to have clustered FoxA binding sites. This, with the fact that 13 genes expressed in the a-line do not have TGTTT repeats, could indicate that *FoxA* is not the only anterior determinant and that other factors trigger gene expression in this domain.

Clustered FoxA binding sites were previously shown to flank the *Ci-sFRP1/5* gene (Lamy et al., 2006). *Ci-Rora/b* and *Ci-sFRP1/5* are members of WNT pathways and show a similar expression pattern at early stages. Interestingly, FoxA clusters were also found in front of the *Ci-ADMP* gene (ci0100135828), which shows a similar anterior-restricted expression pattern in the ectoderm at gastrula stages. *Ci-ADMP* belongs to a family of TGF receptors, which is known to modulate the TGFbeta and BMP pathways in vertebrate anterior nervous system (Willot et al., 2002).

In ascidians, as in vertebrates, anterior ectoderm cells would be protected from posteriorizing signals caudalizing the neurectoderm (Hudson et al., 2003). This protection could occur through the activation of *sFRP1/5*, an antagonist of the canonical Wnt pathway (Dennis et al., 1999) and of other modulators such as ROR (Forrester et al., 2004) or ADMP genes, inhibitors of the BMP pathway (Willot et al., 2002). Moreover, although no direct interaction was proven, another data in line with the involvement of *FoxA* in the regulation of different signalling pathways in anterior ectoderm is that *Ci-Nodal* expression in the anterior ectoderm is repressed by *soxC* and *FoxA* (Imai et al., 2006).

So we can propose that *FoxA* modulates many signalling pathways by co-regulating several actors of these pathways. Thus *FoxA* appears as a major regulator of anterior ectoderm specification. Detailed analysis of the *cis*-regulatory logics of the FoxA targets in a simple chordate model organism should lead to a better understanding of the roles of FoxA-transcription factors and open the route to a systemic approach of the genetic network downstream of *FoxA*.

Acknowledgments

We are grateful to Agnes Roure and Ute Rothbächer for the generous gift of Gateway vectors. We wish to thank D. Casane for expert support in phylogeny; Carole Deyts, Aurélie Heuzé and Laurent Legendre for exceptional technical assistance. Karine Deschet is acknowledged for her help at early stage of this study, that was supported by INRA and CNRS, the French GIS Institut de la Génomique Marine, the Marine Genomics Network of Excellence (EU-FP6 contract no. GOCE-CT-2004-505403), the ANR project CHOREGNET, and the Plurigenes STREP project LSHG-CT-2005-018673, HA and CL were recipients of fellowships from MRT and ARC. MH was funded by the Plurigenes STREP project LSHG-CT-2005-018673, PL was funded by the French Ministry of Research (ACI programme and GIS 'Génomique Marine'), the 'Transcode' framework 6 STREP European Network and the same grants than JSJ.

Appendix A. Supplementary data

Supplementary data associated with this article can be found, in the online version, at doi:10.1016/j.ydbio.2009.02.018.

References

Abeel, T., Saeys, Y., Rouzé, P., Van de Peer, Y., 2008. ProSOM: core promoter prediction based on unsupervised clustering of DNA physical profiles. Bioinformatics 24, i24–i31.

Bertrand, V., Hudson, C., Caillol, D., Popovici, C., Lemaire, P., 2003. Neural tissue in ascidian embryos is induced by FGF9/16/20, acting via a combination of maternal GATA and Ets transcription factors. Cell 115, 615–627.

Billiard, J., Way, D.S., Seestaller-Wehr, L.M., Moran, R.A., Mangine, A., Bodine, P.V., 2005. The orphan receptor tyrosine kinase Ror2 modulates canonical Wnt signaling in osteoblastic cells. Mol. Endocrinol. 19, 90–101.

Blair, J.E., Hedges, S.B., 2005. Molecular phylogeny and divergence times of deuterostome animals. Mol. Biol. Evol. 22, 2275–2284.

Christiaen, L., Jaszczyszyn, Y., Kerfant, M., Kano, S., Thermes, V., Joly, J.S., 2007. Evolutionary modification of mouth position in deuterostomes. Semin. Cell Dev. Biol. 18, 502–511.

Corbo, J.C., Levine, M., Zeller, R.W., 1997. Characterization of a notochord-specific enhancer from the Brachyury promoter region of the ascidian, *Ciona intestinalis*. Development 124, 589–602.

Dehal, P., Satou, Y., Campbell, R.K., Chapman, J., Degnan, B., De Tomaso, A., Davidson, B., Di Gregorio, A., Gelpke, M., Goodstein, D.M., Harafuji, N., Hastings, K.E., Ho, I., Hotta, K., Huang, W., Kawashima, T., Lemaire, P., Martinez, D., Meinertzhagen, I.A., Necula, S., Nonaka, M., Putnam, N., Rash, S., Saiga, H., Satake, M., Terry, A., Yamada, L., Wang, H.G., Awazu, S., Azumi, K., Boore, J., Branno, M., Chin-Bow, S., DeSantis, R., Doyle, S., Francino, P., Keys, D.N., Haga, S., Hayashi, H., Hino, K., Imai, K.S., Inaba, K., Kano, S., Kobayashi, K., Kobayashi, M., Lee, B.I., Makabe, K.W., Manohar, C., Matassi, G., Medina, M., Mochizuki, Y., Mount, S., Morishita, T., Miura, S., Nakayama, A., Nishizaka, S., Nomoto, H., Ohta, F., Oishi, K., Rigoutsos, I., Sano, M., Sasaki, A., Sasakura, Y., Shoguchi, E., Shin-i, T., Spagnuolo, A., Stainier, D., Suzuki, M.M., Tassy, O., Takatori, N., Tokuoka, M., Yagi, K., Yoshizaki, F., Wada, S., Zhang, C., Hyatt, P.D., Larimer, F., Detter, C., Doggett, N., Glavina, T., Hawkins, T., Richardson, P., Lucas, S., Kohara, Y., Levine, M., Satoh, N., Rokhsar, D.S., 2002. The draft genome of *Ciona intestinalis*: insights into chordate and vertebrate origins. Science 298, 2157–2167.

Delsuc, F., Brinkmann, H., Chourrout, D., Philippe, H., 2006. Tunicates and not cephalochordates are the closest living relatives of vertebrates. Nature 439, 965–968.

Dennis, S., Aikawa, M., Szeto, W., d'Amore, P.A., Papkoff, J., 1999. A secreted frizzled related protein, FrzA, selectively associates with Wnt-1 protein and regulates wnt-1 signaling. J. Cell. Sci. 112, 3815–3820.

Deyts, C., Candal, E., Joly, J.S., Bourrat, F., 2005. An automated in situ hybridization screen in the medaka to identify unknown neural genes. Dev. Dyn. 234, 698–708.

Forrester, W.C., Kim, C., Garriga, G., 2004. The *Caenorhabditis elegans* Ror RTK CAM-1 inhibits EGL-20/Wnt signaling in cell migration. Genetics 168, 1951–1962.

Frazer, K.A., Pachter, L., Poliakov, A., Rubin, E.M., Dubchak, I., 2004. VISTA: computational tools for comparative genomics. Nucleic Acids Res. 32, W273–279.

Gaudet, J., Mango, S.E., 2002. Regulation of organogenesis by the *Caenorhabditis elegans* FoxA protein PHA-4. Science 295, 821–825.

Green, J., Inoue, T., Sternberg, P., 2007. The *C. elegans* ROR receptor tyrosine kinase, CAM-1, non-autonomously inhibits the Wnt pathway. Development 134, 4053–4062.

Guindon, S., Gascuel, O., 2003. A simple, fast, and accurate algorithm to estimate large phylogenies by maximum likelihood. Syst. Biol. 52, 696–704.

Hikasa, H., Shibata, M., Hiratani, I., Taira, M., 2002. The *Xenopus* receptor tyrosine kinase Xror2 modulates morphogenetic movements of the axial mesoderm and neuroectoderm via Wnt signaling. Development 129, 5227–5239.

Hotta, K., Mitsuhara, K., Takahashi, H., Inaba, K., Oka, K., Gojobori, T., Ikeo, K., 2007. A web-based interactive developmental table for the ascidian *Ciona intestinalis*, including 3D real-image embryo reconstructions: I. From fertilized egg to hatching larva. Dev. Dyn. 236, 1790–1805.

Hudson, C., Lemaire, P., 2001. Induction of anterior neural fates in the ascidian *Ciona intestinalis*. Mech. Dev. 100, 189–203.

Hudson, C., Darras, S., Caillol, D., Yasuo, H., Lemaire, P., 2003. A conserved role for the MEK signalling pathway in neural tissue specification and posteriorisation in the invertebrate chordate, the ascidian *Ciona intestinalis*. Development 130, 147–159.

Hughes, J.D., Estep, P.W., Tavazoie, S., Church, G.M., 2000. Computational identification of cis-regulatory elements associated with groups of functionally related genes in *Saccharomyces cerevisiae*. J. Mol. Biol. 296, 1205–1214.

Imai, K., Hino, K., Yagi, K., Satoh, N., Satou, Y., 2004. Gene expression profiles of transcription factors and signaling molecules in the ascidian embryo: towards a comprehensive understanding of gene networks. Development 131, 4047–4058.

Imai, K., Levine, M., Satoh, N., Satou, Y., 2006. Regulatory blueprint for a chordate embryo. Science 312, 1183–1187.

Jaillon, O., Aury, J.M., Brunet, F., Petit, J.L., Stange-Thomann, N., Mauceli, E., Bouneau, L., Fischer, C., Ozouf-Costaz, C., Bernot, A., Nicaud, S., Jaffe, D., Fisher, S., Lutfalla, G., Dossat, C., Segurens, B., Dasilva, C., Salanoubat, M., Levy, M., Boudet, N., Castellano, S., Anthouard, V., Jubin, C., Castelli, V., Katinka, M., Vacherie, B., Biémont, C., Skalli, Z., Cattolico, L., Poulain, J., De Berardinis, V., Cruaud, C., Duprat, S., Brottier, P., Coutanceau, J.P., Gouzy, J., Parra, G., Lardier, G., Chapple, C., McKernan, K.J., McEwan, P., Bosak, S., Kellis, M., Volff, J.N., Guigó, R., Zody, M.C., Mesirov, J., Lindblad-Toh, K., Birren, B., Nusbaum, C., Kahn, D., Robinson-Rechavi, M., Laudet, V., Schachter, V., Quétier, F., Saurin, W., Scarpelli, C., Wincker, P., Lander, E.S., Weissenbach, J., Roest

Crollius, H., 2004. Genome duplication in the teleost fish Tetraodon nigroviridis reveals the early vertebrate proto-karyotype. Nature 431, 946–957.
Kiecker, C., Niehrs, C., 2001. A morphogen gradient of Wnt/beta-catenin signalling regulates anteroposterior neural patterning in *Xenopus*. Development 128, 4189–4201.
Lamy, C., Rothbächer, U., Caillol, D., Lemaire, P., 2006. Ci-FoxA-a is the earliest zygotic determinant of the ascidian anterior ectoderm and directly activates Ci-sFRP1/5. Development 133, 2835–2844.
Lemaire, P., Smith, W.C., Nishida, H., 2008. Ascidians and the plasticity of the chordate developmental program. Curr. Biol. 18, 620–631.
Li, C., Chen, H., Hu, L., Xing, Y., Sasaki, T., Villosis, M., Li, J., Nishita, M., Minami, Y., Minoo, P., 2008. Ror2 modulates the canonical Wnt signaling in lung epithelial cells through cooperation with Fzd2. BMC Mol. Biol. 9, 11.
Liu, G., Bafico, A., Aaronson, S.A., 2005. The mechanism of endogenous receptor activation functionally distinguishes prototype canonical and noncanonical Wnts. Mol. Cell Biol. 25, 3475–3482.
Matsuda, T., Nomi, M., Ikeya, M., Kani, S., Oishi, I., Terashima, T., Takada, S., Minami, Y., 2001. Expression of the receptor tyrosine kinase genes, Ror1 and Ror2, during mouse development. Mech. Dev. 105, 153–156.
Matys, V., Fricke, E., Geffers, R., Gässling, E., Haubrock, M., Hehl, R., Hornischer, K., Karas, D., Kel, A.E., Kel-Margoulis, O.V., Kloos, D.U., Land, S., Lewicki-Potapov, B., Michael, H., Münch, R., Reuter, I., Rotert, S., Saxel, H., Scheer, M., Thiele, S., Wingender, E., 2003. TRANSFAC: transcriptional regulation, from patterns to profiles. Nucleic Acids Res. 31, 374–378.
Mikels, A.J., Nusse, R., 2006a. Purified Wnt5a protein activates or inhibits beta-catenin-TCF signaling depending on receptor context. PLoS Biol. 4, e115.
Mikels, A.J., Nusse, R., 2006b. Wnts as ligands: processing, secretion and reception. Oncogene 25, 7461–7468.
Mita-Miyazawa, I., Ikegami, S., Satoh, N., 1985. Histospecific acetylcholinesterase development in the presumptive muscle cells isolated from 16-cell-stage ascidian embryos with respect to the number of DNA replications. J. Embryol. Exp. Morphol. 87, 1–12.
Nishida, H., Satoh, N., 1985. Cell lineage analysis in ascidian embryos by intracellular injection of a tracer enzyme. II. The 16- and 32-cell stages. Dev. Biol. 110, 440–454.
Oishi, I., Suzuki, H., Onishi, N., Takada, R., Kani, S., Ohkawara, B., Koshida, I., Suzuki, K., Yamada, G., Schwabe, G.C., Mundlos, S., Shibuya, H., Takada, S., Minami, Y., 2003. The receptor tyrosine kinase Ror2 is involved in non-canonical Wnt5a/JNK signalling pathway. Genes Cells 8, 645–654.
Okado, H., Takahashi, K., 1990. Induced neural-type differentiation in the cleavage-arrested blastomere isolated from early ascidian embryos. J. Physiol. 427, 603–623.
Overdier, D.G., Porcella, A., Costa, R.H., 1994. The DNA-binding specificity of the hepatocyte nuclear factor 3/forkhead domain is influenced by amino-acid residues adjacent to the recognition helix. Mol. Cell. Biol. 14, 2755–2766.
Passamaneck, Y.J., Hadjantonakis, A.K., Di Gregorio, A., 2007. Dynamic and polarized muscle cell behaviors accompany tail morphogenesis in the ascidian *Ciona intestinalis*. PLoS ONE 2, 714.
Philippe, H., 1993. MUST, a computer package of Management Utilities for Sequences and Trees. Nucleic Acids Res. 21, 5264–5272.
Polakis, P., 1997. The adenomatous polyposis coli (APC) tumor suppressor. Biochem. Biophys. Acta 1332, F127–147.
Polakis, P., 2007. The many ways of Wnt in cancer. Curr. Opin. Genet. Dev. 17, 45–51.
Reya, T., Clevers, H., 2005. Wnt signalling in stem cells and cancer. Nature 434, 843–850.
Rose, S.M., 1939. Embryonic induction in the ascidia. Biol. Bull. Mar. Biol. 77, 216–232.
Roure, A., Rothbächer, U., Robin, F., Kalmar, E., Ferone, G., Lamy, C., Missero, C., Mueller, F., Lemaire, P., 2007. A multicassette Gateway vector set for high throughput and comparative analyses in ciona and vertebrate embryos. PLoS ONE 2, e916.
Saitou, N., Nei, M., 1987. The neighbor-joining method: a new method for reconstructing phylogenetic trees. Mol. Biol. Evol. 4, 406–425.
Satoh, N., Jeffery, W.R., 1995. Chasing tails in ascidians: developmental insights into the origin and evolution of chordates. Trends Genet. 11, 354–359.
Satou, Y., Yamada, L., Mochizuki, Y., Takatori, N., Kawashima, T., Sasaki, A., Hamaguchi, M., Awazu, S., Yagi, K., Sasakura, Y., Nakayama, A., Ishikawa, H., Inaba, K., Satoh, N., 2002. A cDNA resource from the basal chordate *Ciona intestinalis*. Genesis 33, 153–154.
Satou, Y., Hamaguchi, M., Takeuchi, K., Hastings, K.E., Satoh, N., 2006. Genomic overview of mRNA 5′-leader trans-splicing in the ascidian *Ciona intestinalis*. Nucleic Acids Res. 34, 3378–3388.
Thermes, V., Grabher, C., Ristoratore, F., Bourrat, F., Choulika, A., Wittbrodt, J., Joly, J.S., 2002. I-SceI meganuclease mediates highly efficient transgenesis in fish. Mech. Dev. 118, 91–98.
Thompson, J.D., Gibson, T.J., Plewniak, F., Jeanmougin, F., Higgins, D.G., 1997. The CLUSTAL_X windows interface: flexible strategies for multiple sequence alignment aided by quality analysis tools. Nucleic Acids Res. 25, 4876–4882.
Vinson, J.P., Jaffe, D.B., O'Neill, K., Karlsson, E.K., Stange-Thomann, N., Anderson, S., Mesirov, J.P., Satoh, N., Satou, Y., Nusbaum, C., Birren, B., Galagan, J.E., Lander, E.S., 2005. Assembly of polymorphic genomes: algorithms and application to *Ciona savignyi*. Genome Res. 15, 1127–1135.
Willot, V., Mathieu, J., Lu, Y., Schmid, B., Sidi, S., Yan, Y.L., Postlethwait, J.H., Mullins, M., Rosa, F., Peyrieras, N., 2002. Cooperative action of ADMP- and BMP-mediated pathways in regulating cell fates in the zebrafish gastrula. Dev. Biol. 241, 59–78.
Yoda, A., Oishi, I., Minami, Y., 2003. Expression and function of the Ror-family receptor tyrosine kinases during development: lessons from genetic analyses of nematodes, mice, and humans. J. Recept. Signal Transduct. Res. 23, 1–15.